ACS OMEGA

Open Access

http://pubs.acs.org/journal/acsodf

Article

Green Synthesis of PtPdNiFeCu High-Entropy Alloy Nanoparticles for Glucose Detection

Fengxia Wang,* Xin Feng, Yanting Gao, Xu Ding, Wei Wang, and Ji Zhang

Cite This: *ACS Omega* 2023, 8, 47773−47780

Read Online

ACCESS | Metrics & More | Article Recommendations

ABSTRACT: High-entropy alloys have long been used as a new type of alloy material and have attracted widespread concern because of their excellent performance, including their stable microstructure and particular catalytic properties. To design a safer preparation method, we report a novel approach targeting green synthesis, using tea polyphenols to prepare PtPdNiFeCu high-entropy alloy nanoparticles for glucose detection. The fabricated sensors were characterized by transmission electron microscopy and electrochemical experiments. Physical characterization showed that the nanoparticle has better dispersibility, and the average particle size is 7.5 nm. The electrochemical results showed that Tp-PtPdNiFeCu HEA-NPs had a high sensitivity of 1.264 μA mM^{-1} cm^{-2}, a low detection limit of 4.503 μM, and a wide detection range of 0 - 10 mM. In addition, the sensor has better stability and selectivity for glucose detection.

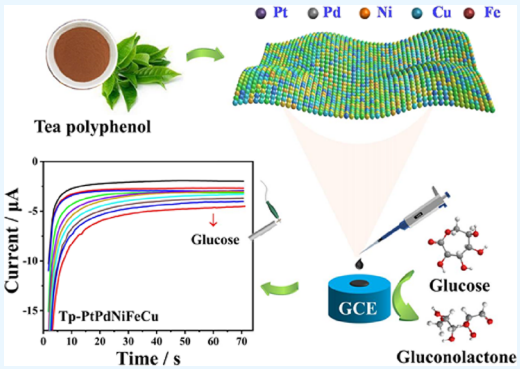

1. INTRODUCTION

Glucose is a kind of polyhydroxy aldehyde, which is one of the most widely distributed and important monosaccharides in nature.[1] Glucose is not only the main energy source of the human body, but also one of the main components of most foods.[2,3] In the human body, the imbalance of glucose in the blood will lead to a series of diseases, such as diabetes, hypoglycemia, decreased glucose tolerance, and decreased fasting blood sugar, posing a great threat to human life.[4,5] In the food industry, testing the glucose content of foods and beverages can not only control glucose intake, but also further monitor blood sugar levels.[6] In addition, the detection of glucose also helps to monitor and control the content of additives in food, thus ensuring the safety and quality of food.[7] Therefore, the development of a low-cost, reliable, and efficient glucose sensor has far-reaching social and economic significance.

Among the many methods of glucose detection, the electrochemical method has been widely concerned because of its simple equipment configuration, high sensitivity and reliability, low detection limit, and high cost efficiency.[8] Among them, nonenzyme sensors based on electrocatalysis are considered to be more promising than enzyme sensors because they overcome the limitation of enzyme sensitivity to environmental temperature factors and can continuously detect glucose changes with high performance.[9] Currently, a wide variety of electrocatalyst materials, such as noble metals, alloys, metal oxides, nanocomposites, and carbon-based materials, have been used in the field of electrochemical sensing.[10] Among them, high-entropy alloys (HEAs) are special alloys made from the mixture of five or more metallic elements, with high strength, high hardness, excellent selectivity, good thermodynamic stability, and other properties.[11−13] Compared with other alloys, HEAs can control their catalytic activity through reasonable adjustments in composition, geometry, structure, and size, and are expected to provide better catalytic activity.[14] However, HEAs as catalysts for glucose sensors have not been extensively studied. Therefore, the development of the HEAs series of electrocatalysts has a broad development space, which can promote its development in the field of electrochemistry.

Biosynthesis pathway is a safe, biocompatible, and environmentally friendly green synthesis method. The biological method mainly uses materials such as plants, bacteria, fungi, and algae to synthesize nanoparticles (NPs).[15] Tea polyphenol (Tp) is an extract of tea, containing more than two hydroxyl polyphenols, so it has a strong hydrogen supply capacity.[16−18] In the process of reducing metal NPs with tea polyphenols, polyphenols with hydroxyl groups are oxidized into biological compounds with carbonyl groups (such as quinones), resulting in the reduction of metal ions to metal atoms. Quinones should be attached to the surface of NPs through their

Received: August 18, 2023
Revised: October 14, 2023
Accepted: November 23, 2023
Published: December 6, 2023

carbonyl groups, forming a steric barrier layer and generating a repulsion force, so as to avoid the accumulation of NPs and ensure its stability.[19,20] Therefore, tea polyphenols can be used directly as reducing agent and stabilizer for the synthesis of NPs, without the need to add any additional surfactants or other substances.[21]

In this paper, PtPdNiFeCu HEA-NPs were synthesized in one step with tea polyphenols as green natural raw material, which is a new method for green synthesis of HEAs. When applied to glucose detection, the sensor has the advantages of wide detection range, high sensitivity, a low detection limit, good stability, and selectivity.

2. EXPERIMENT

2.1. Chemicals and Materials. Tea polyphenols (Tp, purity: 98%; molecular weight: 281.36 g moL^{-1}) was purchased from Jiahe Biological Co., Ltd. Cabot Co., Ltd. provided carbon powder (Vulcan XC-72R) (USA). Nafion solution (USA) was bought from DuPont Co., Ltd. Ferric chloride ($FeCl_3$), nickel chloride ($NiCl_2$), cupric chloride ($CuCl_2$), β-D-glucose, acetamidophenol (AP), sodium chloride (NaCl), and trisodium citrate dihydrate ($C_6H_5Na_3O_7$) were purchased from Aladdin Co., Ltd. Palladium chloride ($PdCl_2$) and chloroplatinic acid ($H_2PtCl_6{\cdot}6H_2O$) were acquired from Koda Reagent Co., Ltd. Ascorbic acid (AA) was bought from Xiya Reagent Co., Ltd. Uric acid (UA) was acquired from Saen Chemical Reagent Co., Ltd. Deionized water was used for all solutions during the experiment. All tests were performed at room temperature.

2.2. Synthesis of Tp-PtPdNiFeCu. For synthesis of PtPdNiFeCu HEA-NPs, equimolar $H_2PtCl_6{\cdot}6H_2O$, $PdCl_2$, $FeCl_3$, $NiCl_2$, and $CuCl_2$ were dissolved in a flask. Then, 124.88 mg carbon powder, 200 mg sodium citrate, and 30 mL tea polyphenols (10 mg mL^{-1}) were added to the above solution. It was stirred continuously for 4 h, then transferred to the reactor and reflected at 180 °C for 4 h. After the solution was cooled to room temperature, it was centrifuged and washed for many times. Next, the sample was placed in a freeze-dryer, removed for grinding after completion of freeze-drying, and finally labeled as Tp-PtPdNiFeCu. The synthesis route for preparing Tp-PtPdNiFeCu HEA-NPs is shown in Scheme 1.

Scheme 1. Schematic Illustration of the Preparation of Tp-PtPdNiFeCu HEA-NPs

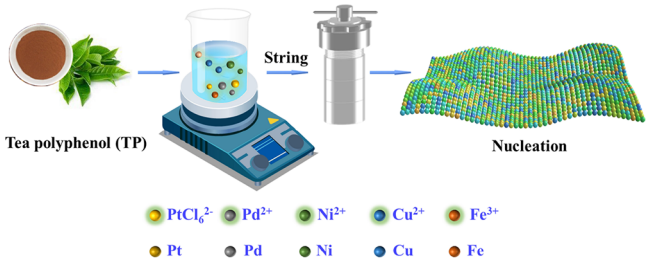

2.3. Characterization. Transmission electron microscopy (TEM, Model: JEOL JEM-2100F, Japan) and selected area electron diffraction (SAED) were used to evaluate the morphology and crystallographic properties of the materials. EDS elemental mapping (X-MaxN 80T IE250) was used to analyze the chemical composition. X-ray photoelectron spectroscopy (XPS) was performed on a monochromatic Al K_α X-ray source (250Xi, America, $h\upsilon$ = 29.35 eV). The crystal structure of the NPs was studied by an X-ray diffractometer (XRD) (Rigaku D/Max-2400, Japan).

The materials' electrochemical tests were conducted by an electrochemical work station (CHI 760E) and Keithley 2400. A standard three-electrode cell was used for electrocatalytic experiments at room temperature. A Pt sheet and Ag/AgCl were used as counter electrode and reference electrode, respectively, and a catalyst-modified glassy carbon electrode (GCE) was used as working electrode. In the electrochemical test, 3.0 mg of the sample was distributed in 0.6 mL of ethanol, which was homogenized by ultrasound. Then, 4 μL sample was dropped on the surface of the GCE (5 mm in diameter). After drying at room temperature, 4 μL sample was added and dried again. Finally, 4 μL of Nafion/ethanol (0.25% Nafion) was added to protect the electrode. Before all tests, the electrolyte was purified with high-purity Ar gas to ensure gas saturation. In this experiment, all potentials were measured according to Ag/AgCl.

3. RESULTS AND DISCUSSION

3.1. Physical Characterizations. First, the morphological characteristics of the synthesized Tp-PtPdNiFeCu HEA-NPs were studied by TEM. As shown in the TEM image in Figure 1a, the black dots in the figure were synthetic PtPdNiFeCu NPs with uniform distribution. Figure 1b is the TEM image with further magnification, from which the shape of PtPdNiFeCu can be more clearly observed, and it was reduced to spherical metal particles by Tp. As shown in Figure 1c, the sizes of Tp-PtPdNiFeCu NPs were statistically analyzed. It was found that the particle size of metal NPs was mainly concentrated in the range of 7 - 8 nm, which provided abundant exposed electrochemical active sites for hydrogen evolution reaction and was conducive to the subsequent application of glucose sensors. As shown in the high-resolution transmission electron microscopy (HRTEM) image of Figure 1d, the lattice fringes of PtPdNiFeCu can be clearly seen, and the lattice spacing is 0.226 and 0.178 nm, respectively, corresponding to the *(111)* and *(200)* lattice planes. Combined with the distance and angle between the lattice planes, we confirm the typical face-centered cubic (*fcc*) structure of HEA-NPs. In addition, the crystal structure of the synthesized sample was studied by SAED. From the image of Figure 1e, the bright and dark diffraction rings of Tp-PtPdNiFeCu can be clearly seen, indicating that the prepared PtPdNiFeCu has a typical *fcc* polycrystalline structure.

The crystal structure of Tp-PtPdNiFeCu HEA-NPs was characterized by X-ray diffraction (XRD) analysis (Figure 1f). The peaks of the *fcc* structure were observed at 40.77°, 47.30°, 69.70°, and 83.47°, corresponding to the *(111)*, *(200)*, *(220)*, and *(311)* planes of the single-phase PtPdNiFeCu HEAs, respectively, where the *(111)* plane was dominant in the alloy. Peaks of pure Ni, Cu, Pt, Pd, and Fe were not observed, indicating that these elements were well mixed in the formed nanostructure. In addition, compared with standard cards of pure Pt (JCPDS-04−0802) and Pd (JCPDS-46−1043), the peaks shifted slightly to higher angles. However, the peaks of large Ni (JCPDS-04−0850) show negative deviation.[22] This meant that the Tp-PtPdNiFeCu HEA-NPs was effectively formed.

In addition, we investigated the elemental distribution of PtPdNiFeCu by high-angle annular dark-field scanning transmission electron microscopy (HAADF-STEM) and energy

https://doi.org/10.1021/acsomega.3c06122
ACS Omega 2023, 8, 47773−47780

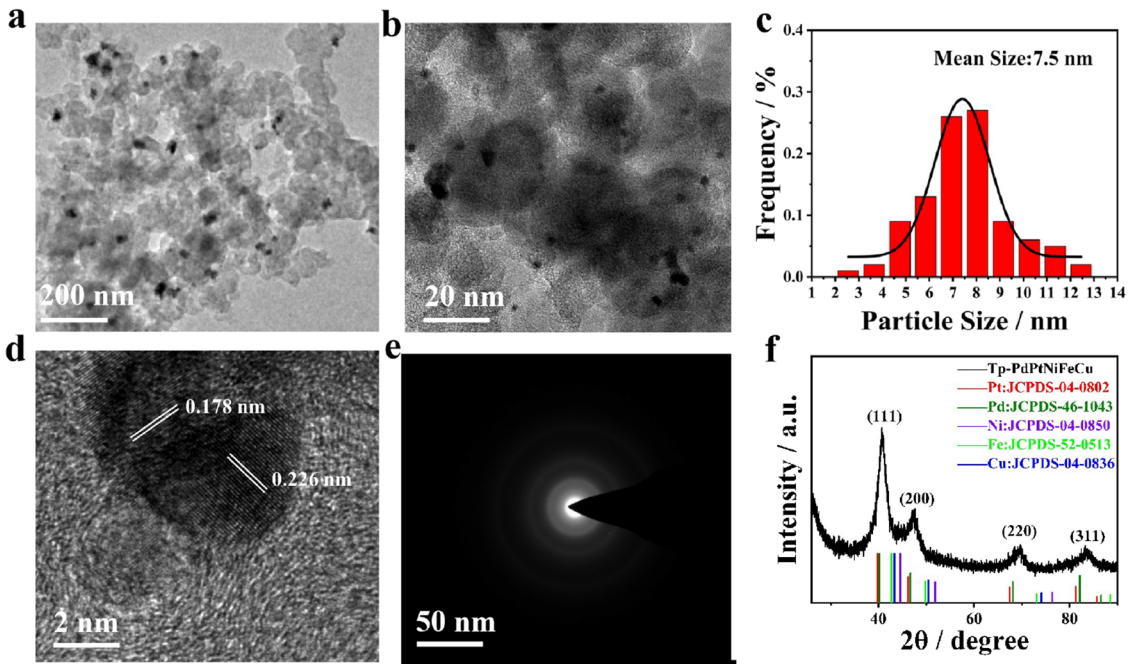

Figure 1. Typical TEM images of Tp-PtPdNiFeCu HEA-NPs electrocatalyst at different bar 200nm (a) and 20nm (b); (c) corresponding particle size distribution histograms; (d) high-resolution TEM image; (e) the corresponding SAED pattern; and (f) XRD patterns of Tp-PtPdNiFeCu HEA-NPs.

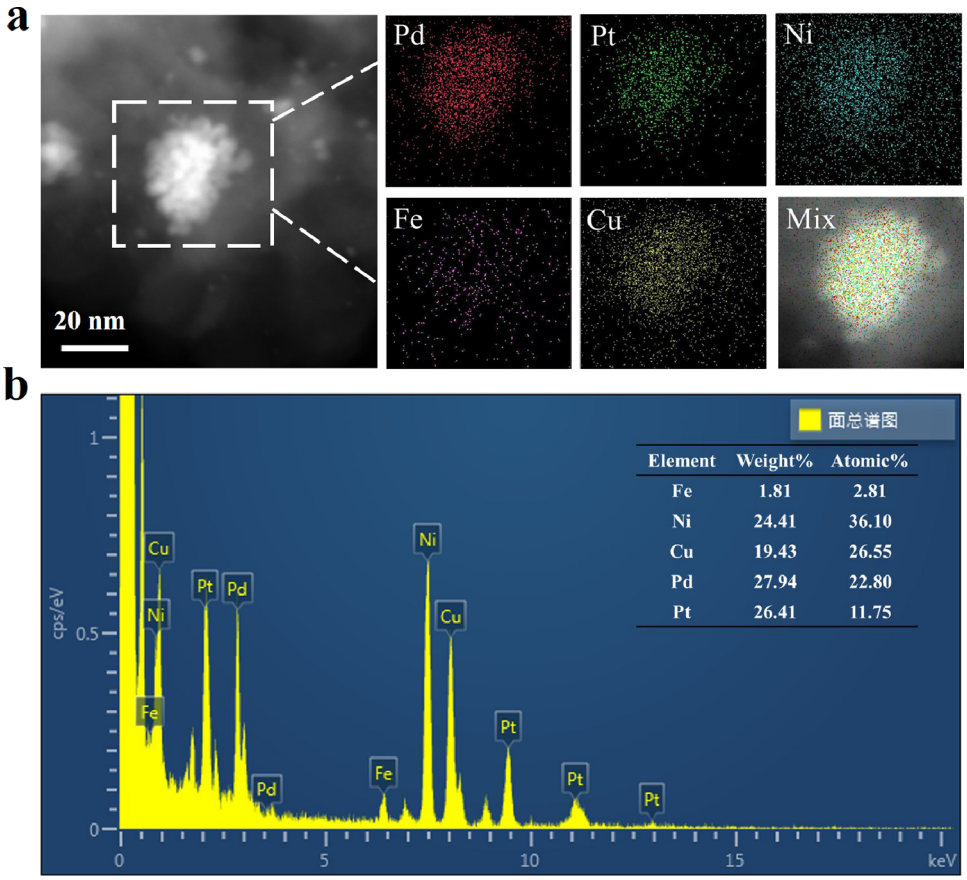

Figure 2. (a) EDS analysis and (b) EDS mapping analysis of PtPdNiFeCu HEA-NPs.

dispersive spectroscopy (EDS). Figure 2a showed the uniform distribution of the elements Pt, Pd, Ni, Fe, and Cu at the atomic scale, and the close contact of each component element on the nanoscale also indicated the formation of PtPdNiFeCu alloy. According to the calculation of EDS (Figure 2b), the Pt,

https://doi.org/10.1021/acsomega.3c06122
ACS Omega 2023, 8, 47773−47780

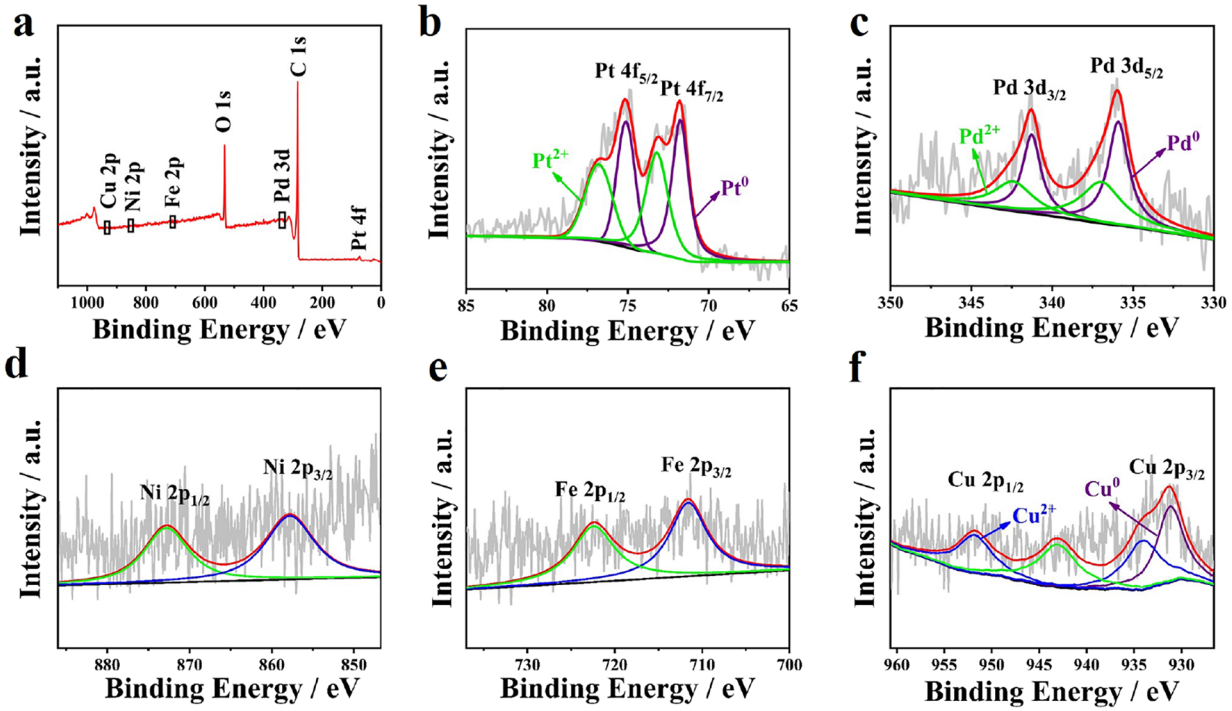

Figure 3. (a) XPS full spectrum of Tp-PtPdNiFeCu HEA-NPs; (b-f) curve-fitted Pt 4f, Pd 3d, Ni 2p, Fe 2p, and Cu 2p.

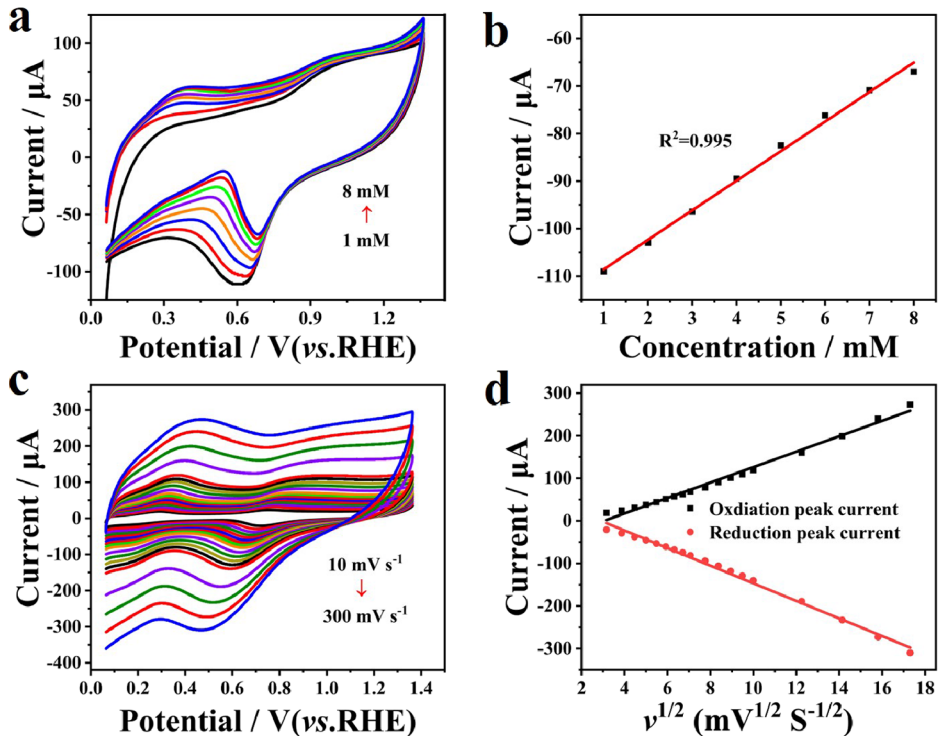

Figure 4. (a) CVs of Tp-PtPdNiFeCu GCE in the Ar-saturated 0.1 M NaOH solution in various concentrations of glucose, scan rate: 50 mV s^{-1}; (b) The calibration curve of the linear dependence of cathodic peak current on the glucose; (c) CV responses of the Tp-PtPdNiFeCu HEA-NPs electrode in 0.1 M NaOH with 1 mM glucose at different scan rates (10, 15, 20, 25, 30, 35, 40, 45, 50, 60, 70, 80, 90, 100, 150, 200, 250, and 300mV s^{-1}); (d) Corresponding linear dependence of peak currents with different scan rates.

Pd, Ni, Fe, and Cu weight ratios were 27.94:26.41:24.41:1.81:19.43, respectively.

The chemical constituents and states of Tp-PtPdNiFeCu were characterized by XPS. Figure 3a is a complete XPS diagram of Tp-PtPdNiFeCu, showing the presence of C1s, O 1s, Pt 4f, Pd 3d, Ni 2p, Fe 2p, and Cu2p. The spectrum of Pt 4f is shown in Figure 3b, the two main peaks at 71.74 and 74.98 eV are designated as the metal Pt0, which is the dominant form of Pt, while the two weaker elements at 73.15 and 76.88 belong to the Pt^{2+} species, and a small amount of Pt^{2+} may also be in the form of PtO or Pt(OH). Meanwhile, the peaks at 335.87 and 341.31 eV in the XPS segment of Pd 4d are shown in

https://doi.org/10.1021/acsomega.3c06122
ACS Omega 2023, 8, 47773−47780

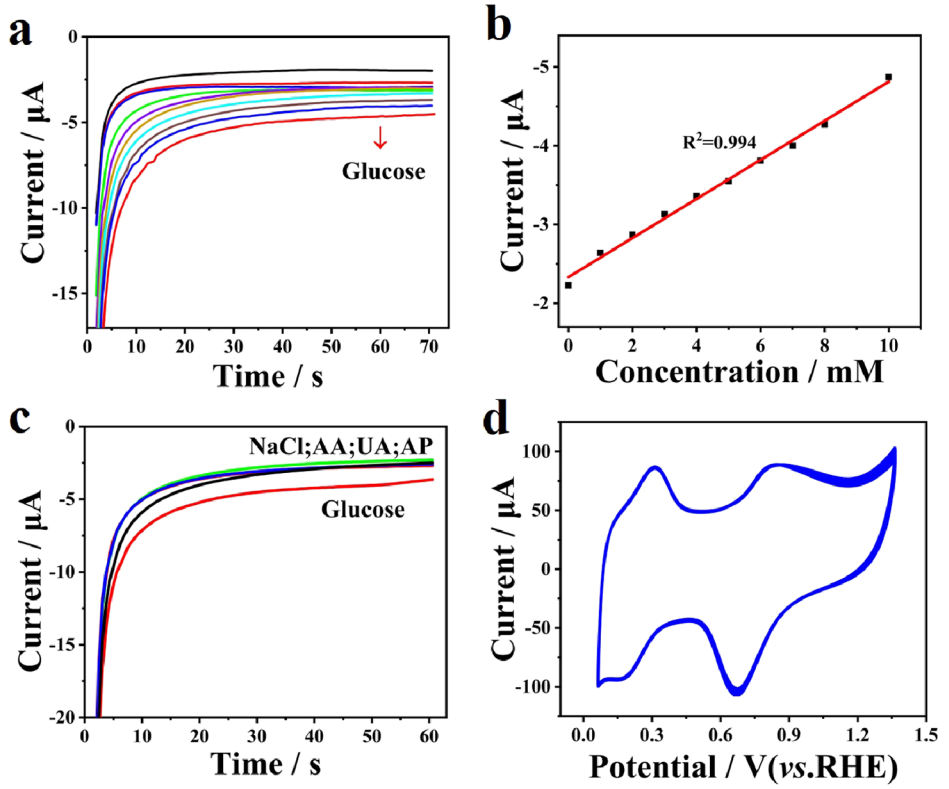

Figure 5. (a) Amperometric response of the Tp-PtPdNiFeCu-modified electrode to successive addition glucose at 0.3 V; (b) Calibration curve of the Tp-PtPdNiFeCu-modified electrode response to different glucose concentrations; (c) Amperometric responses of the Tp-PtPdNiFeCu-modified electrode to successive addition of 0 mM, 2 mM glucose, 0.1 mM AA, 0.1 mM UA, 0.1 mM AP, and 0.1 mM NaCl, detection potential: 0.3 V; (d) CV of the Tp-PtPdNiFeCu-modified electrode in 0.1 M NaOH solution at 1 mM glucose for 50 scans, scan rate: 50 mV s^{-1}.

Figure 3c, while the peaks at 336.93 and 342.47 eV can be fitted to Pd^{2+}. The peaks in Figure 3d belong to Ni $2p_{1/2}$ and Ni $2p_{3/2}$ of Ni^0, which were located at 872.8 and 857.8 eV, respectively. The Fe 2p spectrum in Figure 3e shows that the peaks at 711.59 and 722.42 eV belong to Fe $2p_{3/2}$ and Fe $2p_{1/2}$, respectively. Figure 3f shows the spectrum of Cu 2p. In particular, the dominant peaks of 931.19 and 951.8 eV were from Cu^0, and the dominant peak of 934.09 was from Cu^{2+}. Some of the oxides detected in the high-resolution spectra may be formed by these primary oxides in PtPdNiFeCu HEAs in air or water bath, resulting in the oxidation of surface elements.

3.2. Electrochemical Measurements. The electrocatalytic performance of Tp-PtPdNiFeCu on glucose was detected by cyclic voltammetry (CV) in Ar-saturated solution. As shown in Figure 4a, CV studies were performed at different glucose concentrations (1 - 8 mM) in a 0.1 M NaOH solution at a scanning rate of 50 mV s^{-1}. Apparently, peak oxidation currents (potential of about 0.3 V) were observed after the addition of 1 mM glucose. Moreover, with the increase in glucose concentration, the peak reduction current also increased gradually, which was in good agreement with the current response. Meanwhile, it can be observed from Figure 4b that there was a better linear relationship between glucose concentration and reduction current value, and the linear regression coefficient is 0.995. This may be due to the better synergistic effect between each metal component of PtPdNiFeCu, which improved the detection performance of glucose. Therefore, PtPdNiFeCu nanomaterials have significant electrocatalytic activity on glucose and can be used for glucose detection.

To study the electrochemical kinetics of the catalyst process,[23] CV curves (Figure 4c) at different sweep rates (10 mV s^{-1} - 300 mV s^{-1}) in 1 mM glucose solution were examined. With the increase of scanning rate, the potential of anode and cathode peaks will have positive and negative displacement, while the value of the two peak currents will gradually increase, which was because the reaction kinetics of the internal electrocatalytic process of glucose molecule adsorption was slow due to the higher scanning rate.[24] Meanwhile, it can be observed in Figure 4d that there was a linear relationship between peak current density and the square root of scanning rate, and this indicated that the catalytic process of glucose on the prepared electrode was controlled by diffusion.[25]

The electrochemical performance of the sensor was measured by the amperage response (current−time) of glucose quantitative analysis.[26] As shown in Figure 5a, in the presence of glucose in 0.1 mM NaOH, the current response of PtPdNiFeCu to the continuous addition of 1 mM glucose was tested by potentiostatic testing. In the range of 0 - 10 mM glucose detection, it was found that the absolute value of the increased response current increased with increasing glucose concentration, indicating that PtPdNiFeCu had good electrocatalytic performance and rapid electron exchange ability. As shown in the calibration curve in Figure 5b, there can be a good linear relationship between the glucose concentration and response current (R^2 = 0.994). The corresponding linear equation is expressed as:

$$I(\mu A) = -0.24807C(mM) - 2.332 \quad (1)$$

https://doi.org/10.1021/acsomega.3c06122
ACS Omega 2023, 8, 47773−47780

Table 1. Comparison of the Present Work with Other Studies

catalyst[a]	reduced[b]	sensitivity (μA mM^{-1}cm^{-2})	linear range (mM)	LOD (μM, S/N = 3)	reference
Pt NPs	ED	327	0.1 - 11	0.026	21
Pd NPs	CSP	17.7	1 - 8	237	22
Cu NWs	AA	1001.6	0 - 25	2.3	23
PtPd NPs	EG	1.47	0.1 - 22	2	24
PtPd NPs	EG	52.526	0.1 - 4	1.82	25
PtPd NPs	EG	0.11	1.5 - 12	120	26
PtPd NPs	$NaHSO_3$	112	0.062 - 14.07	31	27
PtNi NPs	DMF	6.67/4.57	0 - 12	21	28
CuPd NPs	ED	298	0.01 - 9.6	0.32	29
CuNi NPs	EG	780	0.001 - 4.1	0.5	30
Cu@NiFe LDH	ED	7.88	0.001 - 0.9	0.1	31
PtPdNiFeCu NPs	Tp	1.264	0 - 10	4.503	this work

[a]NPs = nanoparticle, LDH = layered double hydroxide, and NWs = nanowires. [b]ED = electrodeposite, CSP = *Cynomorium songaricum* polysaccharide, AA = ascorbic acid, EG = ethylene glycol, DMF= dimethylformamide, Tp = tea polyphenols, and AP = acetamido phenol.

The formula of the sensitivity of the sensor electrode can be expressed as:

$$\text{Sensitivity} = A/(C \times \text{area}) \quad (2)$$

where A is the corresponding response current, C is the added glucose concentration in the system, and area is the geometric surface area of a GCE (0.19625 cm^2).[27]

In addition, the limit of detection (LOD) can reasonably determine the lowest detectable concentration of glucose. The formula for calculating LOD can be expressed as follows:

$$\text{LOD} = 3\delta/S \quad (3)$$

δ is the standard deviation and S is the sensitivity.

According to the above formula, the sensitivity of the electrode for glucose detection was 1.264 μA mM^{-1} cm^{-2}, and the detection limit was 4.503 μM (S/N = 3). Meanwhile, the detection range of the prepared PtPdNiFeCu electrode can completely cover the blood glucose range (3 - 8 mM) under normal physiological conditions of the human body, so it can be used for blood glucose detection in the human body. Also, we prepared Table 1 to compare our current work with other studies.[26−36] The results show that the material has a good electrocatalytic response to glucose.

For the glucose sensor electrode, selectivity was an important factor affecting its accuracy. Considering that the real blood environment usually contains endogenous interfering substances, such as UA, AA, metal ions, and other sugars, their presence may affect the sensitivity of glucose sensors.[37] Therefore, we used 2 mM glucose and 0.1 mM AA, UA, AP, and sodium chloride (NaCl) as interfering substances to conduct an interference test on glucose. In Figure 5c, the addition of 0.1 mM AA, UA, DA, AP, and NaCl did not significantly affect the response current. However, when glucose was added to the electrolyte, a higher response current was observed for glucose, indicating that the presence of interfering species did not affect the detection of glucose by PtPdNiFeCu. The results of the selectivity test showed that the PtPdNiFeCu glucose sensor has good selectivity.

For glucose detection, it was important to ensure that the modified electrode had a stable current response to glucose. As shown in Figure 5d, no change in the glucose oxidation peak was observed after 50 consecutive cycles. Obviously, this indicates that the PtPdNiFeCu-modified electrode can produce persistent and stable response current to glucose.

4. CONCLUSIONS

In summary, PtPdNiFeCu HEA-NPs for glucose detection were synthesized using natural Tp. The obtained NPs have good dispersion and a small particle size. Tp-PtPdNiFeCu HEA-NPs showed high sensitivity and good stability in glucose detection, with a wide linear range of 0 - 10 mM, a low detection limit of 4.503 μM, and a high sensitivity of 1.264 μA mM^{-1} cm^{-2}. In addition, Tp-PtPdNiFeCu HEA-NPs could resist the interference of AA, AP, UA, and NaCl. Therefore, this experiment indicates that the synthesis of HEA-NPs in a green manner has a potential application value for glucose detection.

AUTHOR INFORMATION

Corresponding Author

Fengxia Wang − *College of Life Science, Northwest Normal University, Lanzhou 730070, China;* orcid.org/0000-0002-0931-7616; Phone: +86 0931 7971830; Email: wangfx@nwnu.edu.cn

Authors

Xin Feng − *College of Life Science, Northwest Normal University, Lanzhou 730070, China*

Yanting Gao − *College of Life Science, Northwest Normal University, Lanzhou 730070, China*

Xu Ding − *College of Life Science, Northwest Normal University, Lanzhou 730070, China*

Wei Wang − *School of Chemistry and Chemical Engineering, Lanzhou Jiaotong University, Lanzhou 730070, China*

Ji Zhang − *Bioactive Products Engineering Research Center for Gansu Distinctive Plants, Northwest Normal University, Lanzhou 730070, China*

Complete contact information is available at: https://pubs.acs.org/10.1021/acsomega.3c06122

Author Contributions

F.W.: validation, formal analysis, visualization, resources, review, and editing. X.F: physical and electrochemical analysis, software, investigation, writing - original draft, and data curation. Y.G.: formal analysis and visualization. X.D.: formal analysis, writing - review and editing. W.W.: writing - review and editing. J.Z.: resources, writing-review, and editing.

Notes

The authors declare no competing financial interest.

https://doi.org/10.1021/acsomega.3c06122
ACS Omega 2023, 8, 47773−47780

■ ACKNOWLEDGMENTS

This work was supported by the National Natural Science Foundation of China (22161042) and Program for Youth Innovation and Entrepreneurship of Gansu province (2022LQTD15).

■ REFERENCES

(1) Huanan, G.; Shiqin, D.; Qiaoyan, W.; Qi, Z.; Hua, Y.; Dongxu, W. Rapid and sensitive smartphone non-enzymatic colorimetric assay for the detection of glucose in food based on peroxidase-like activity of Fe_3O_4@Au nanoparticles. *Spectrochim Acta A Mol Biomol Spectrosc.* **2023**, *302*, No. 122970.

(2) Dong, Q.; Ling, C.; Zhao, S.; Tang, X.; Zhang, Y.; Xing, Y.; Yu, H.; Huang, K.; Zou, Z.; Xiong, X. One-step rapid synthesis of $Ni_{0.5}Co_{0.5}$-CPO-27 nanorod array with oxygen vacancies based on DBD microplasma: As an effective non-enzymatic glucose sensor for beverage and human serum. *Food Chem.* **2023**, *407*, No. 135144.

(3) Shen, J.; Zhu, C.; Li, L.; Yang, T.; Wu, Y.; Ma, C.; Gu, J.; Gao, H.; Yang, Z.; Wang, Z.; Qiu, X.; Zhong, L.; Hu, A.; Huang, A.; Xu, J.; Guo, S.; Yin, W.; Chen, G. TMB-AgNPs@COF based SERS probe for the rapid detection of glucose in drinks. *Vibrational Spectroscopy.* **2022**, *122*, No. 103411.

(4) Yao, Y.; Chen, J.; Guo, Y.; Lv, T.; Chen, Z.; Li, N.; Cao, S.; Chen, B.; Chen, T. Integration of interstitial fluid extraction and glucose detection in one device for wearable non-invasive blood glucose sensors. *Biosensors and Bioelectronics.* **2021**, *179*, No. 113078.

(5) Wei, L.; Ding, J.; Wu, J.; Li, L.; Li, Q.; Shao, L.-X.; Lu, J.; Qian, J. An efficient glucose sensor thermally calcined from copper-organic coordination cages. *Talanta.* **2022**, *241*, No. 123263.

(6) He, L.; Su, J.; You, T.; Xiao, S.; Shen, Y.; Jiang, P.; He, D. Mn incorporation boosted NiO nanosheets as highly efficient anode for sensitive glucose detection in beverage. *LWT* **2023**, *182*, 114801.

(7) Cao, B.; Gao, G.; Zhang, J.; Zhang, Z.; Sun, T. A smartphone-assisted colorimetric sensor based on Fe1-xS nanozyme for detection of glucose and ascorbic-acid in soft drinks. *Microchemical Journal.* **2023**, *193*, No. 109018.

(8) Alghazzawi, W.; Danish, E.; Alnahdi, H.; Salam, M. A. Rapid microwave-assisted hydrothermal green synthesis of rGO/NiO nanocomposite for glucose detection in diabetes. *Synth. Met.* **2020**, *267*, No. 116401, DOI: 10.1016/j.synthmet.2020.116401.

(9) Liu, X.; Zhou, X.; Yang, C.; Yang, W.; Liu, G.; Li, Y.; Zhang, G.; Zhao, X. Surfactant-free synthesis of CuBr NPs decorated by Pt for glucose and nitrite sensors. *Journal of Industrial and Engineering Chemistry.* **2023**, *124*, 323−330.

(10) Solhi, M.; Rahsepar, M.; Kazemi Asl, A. A.; Kim, H. Synthesis and characterization of a high-performance enzyme-free glucose sensor based on mesoporous copper oxide nanoparticles. *Mater. Res. Bull.* **2023**, *164*, No. 112240.

(11) Katiyar, N. K.; Biswas, K.; Yeh, J.-W.; Sharma, S.; Tiwary, C. S. A perspective on the catalysis using the high entropy alloys. *Nano Energy* **2021**, *88*, No. 106261.

(12) Qiu, H.-J.; Fang, G.; Wen, Y.; Liu, P.; Xie, G.; Liu, X.; Sun, S. Nanoporous high-entropy alloys for highly stable and efficient catalysis. *Journal of Materials Chemistry A.* **2019**, *7*, 6499−6506.

(13) Gawel, R.; Rogal, Ł.; Dąbek, J.; Wójcik-Bania, M.; Przybylski, K. High temperature oxidation behaviour of non-equimolar AlCoCrFeNi high entropy alloys. *Vacuum.* **2021**, *184*, No. 109969.

(14) Buckingham, M. A.; Ward-O'Brien, B.; Xiao, W.; Li, Y.; Qu, J.; Lewis, D. J. High entropy metal chalcogenides: synthesis, properties, applications and future directions. *Chem Commun (Camb).* **2022**, *58* (58), 8025−8037.

(15) Alshameri, A. W.; Owais, M. Antibacterial and cytotoxic potency of the plant-mediated synthesis of metallic nanoparticles Ag NPs and ZnO NPs: A review. *OpenNano.* **2022**, *8*, No. 100077.

(16) Onitsuka, S.; Hamada, T.; Okamura, H. Preparation of antimicrobial gold and silver nanoparticles from tea leaf extracts. *Colloids Surf. B: Biointerfaces* **2018**, *173*, 242−248, DOI: 10.1016/j.colsurfb.2018.09.055.

(17) Xiao, C.; Li, H.; Zhao, Y.; Zhang, X.; Wang, X. Green synthesis of iron nanoparticle by tea extract (polyphenols) and its selective removal of cationic dyes. *J Environ Manage.* **2020**, *275*, No. 111262.

(18) Jadoun, S.; Arif, R.; Jangid, N. K.; Meena, R. K. Green synthesis of nanoparticles using plant extracts: a review. *Environ. Chem. Lett.* **2020**, *19*, 355−374, DOI: 10.1007/s10311-020-01074-x.

(19) Cassani, L.; Marcovich, N. E.; Gomez-Zavaglia, A. Seaweed bioactive compounds: Promising and safe inputs for the green synthesis of metal nanoparticles in the food industry. *Crit. Rev. Food Sci. Nutr.* **2021**, *63*, 1527−1550, DOI: 10.1080/10408398.2021.1965537.

(20) Ahmad, T.; Bustam, M. A.; Irfan, M.; Moniruzzaman, M.; Asghar, H. M. A.; Bhattacharjee, S. Mechanistic investigation of phytochemicals involved in green synthesis of gold nanoparticles using aqueous Elaeis guineensis leaves extract: Role of phenolic compounds and flavonoids. *Biotechnology and Applied Biochemistry.* **2019**, *66* (4), 698−708.

(21) Siddiqi, K. S.; Husen, A. Fabrication of Metal and Metal Oxide Nanoparticles by Algae and their Toxic Effects. *Nanoscale Res. Lett.* **2016**, *11* (1), 363.

(22) Feng, Y.-G.; Niu, H.-J.; Mei, L.-P.; Feng, J.-J.; Fang, K.-M.; Wang, A.-J. Engineering 3D hierarchical thorn-like PtPdNiCu alloyed nanotripods with enhanced performances for methanol and ethanol electrooxidation. *J. Colloid Interface Sci.* **2020**, *575*, 425−532.

(23) Lin, S.; Feng, W.; Miao, X.; Zhang, X.; Chen, S.; Chen, Y.; Wang, W.; Zhang, Y. A flexible and highly sensitive nonenzymatic glucose sensor based on DVD-laser scribed graphene substrate. *Biosensors and Bioelectronics.* **2018**, *110*, 89−96.

(24) Zhang, Y.; Li, N.; Xiang, Y.; Wang, D.; Zhang, P.; Wang, Y.; Lu, S.; Xu, R.; Zhao, J. A flexible non-enzymatic glucose sensor based on copper nanoparticles anchored on laser-induced graphene. *Carbon* **2020**, *56*, 506−513.

(25) Sun, F.; Wang, X.; You, Z.; Xia, H.; Wang, S.; Jia, C.; Zhou, Y.; Zhang, J. Sandwich structure confined gold as highly sensitive and stable electrochemical non-enzymatic glucose sensor with low oxidation potential. *Journal of Materials Science & Technology.* **2022**, *123*, 113−122.

(26) Rafique, N.; Asif, A. H.; Hirani, R. A. K.; Wu, H.; Shi, L.; Zhang, S.; Sun, H. Binder free 3D core−shell NiFe layered double hydroxide (LDH) nanosheets (NSs) supported on Cu foam as a highly efficient non-enzymatic glucose sensor. *J. Colloid Interface Sci.* **2022**, *615*, 865−875.

(27) Wang, F.; Niu, X.; Wang, W.; Jing, W.; Huang, Y.; Zhang, J. Green synthesis of Pd nanoparticles via extracted polysaccharide applied to glucose detection. *Journal of the Taiwan Institute of Chemical Engineers.* **2018**, *93*, 87−93.

(28) Malhotra, S.; Tang, Y.; Varshney, P. K. Fabrication of highly sensitive non-enzymatic sensor based on Pt/PVF modified Pt electrode for detection of glucose. *Journal of the Iranian Chemical Society.* **2020**, *17* (3), 521−531.

(29) Liu, X.; Yang, C.; Yang, W.; Lin, J.; Liang, C.; Zhao, X. One-pot synthesis of uniform Cu nanowires and their enhanced non-enzymatic glucose sensor performance. *J. Mater. Sci.* **2021**, *56* (9), 5520−5531.

(30) Li, M.; Bo, X.; Zhang, Y.; Han, C.; Guo, L. One-pot ionic liquid-assisted synthesis of highly dispersed PtPd nanoparticles/reduced graphene oxide composites for nonenzymatic glucose detection. *Biosens Bioelectron.* **2014**, *56*, 223−230.

(31) Salah, A.; Al-Ansi, N.; Adlat, S.; Bawa, M.; He, Y.; Bo, X.; Guo, L. Sensitive nonenzymatic detection of glucose at PtPd/porous holey nitrogen-doped graphene. *J. Alloys Compd.* **2019**, *792*, 50−58.

(32) Bo, X.; Bai, J.; Yang, L.; Guo, L. The nanocomposite of PtPd nanoparticles/onion-like mesoporous carbon vesicle for nonenzymatic amperometric sensing of glucose. *Sensors and Actuators B: Chemical.* **2011**, *157* (2), 662−668.

(33) Chen, K. J.; Lee, C. F.; Rick, J.; Wang, S. H.; Liu, C. C.; Hwang, B. J. Fabrication and application of amperometric glucose biosensor based on a novel PtPd bimetallic nanoparticle decorated multi-walled carbon nanotube catalyst. *Biosens Bioelectron.* **2012**, *33* (1), 75−81.

(34) Najmi, A.; Saidi, M. S.; Shahrokhian, S.; Hosseini, H.; Hannani, S. K. Fabrication of a microdialysis-based nonenzymatic microfluidic sensor for regular glucose measurement. *Sens. Actuators: B. Chem.* **2021**, *333*, No. 129569.
(35) Li, Z.-H.; Zhao, X.-L.; Jiang, X.-C.; Wu, Y.-H.; Chen, C.; Zhu, Z.-G.; Marty, J.-L.; Chen, Q.-S. An enhanced Nonenzymatic Electrochemical Glucose Sensor Based on Copper-Palladium Nanoparticles Modified Glassy Carbon Electrodes. *Electroanalysis.* **2018**, *30* (8), 1811−1819.
(36) Wu, K.-L.; Cai, Y.-M.; Jiang, B.-B.; Cheong, W.-C.; Wei, X.-W.; Wang, W.; Yu, N. Cu@Ni core−shell nanoparticles/reduced graphene oxide nanocomposites for nonenzymatic glucose sensor. *RSC Advances.* **2017**, *7* (34), 21128−21135.
(37) Liu, W.; Zhao, X.; Dai, Y.; Qi, Y. Study on the oriented self-assembly of cuprous oxide micro-nano cubes and its application as a non-enzymatic glucose sensor. *Colloids Surf. B: Biointerfaces* **2022**, *211*, No. 112317.

https://doi.org/10.1021/acsomega.3c06122
ACS Omega 2023, 8, 47773−47780